PERIODICO di MINERALOGIA
established in 1930

DIPARTIMENTO
DI SCIENZE DELLA TERRA

SAPIENZA
UNIVERSITÀ DI ROMA

An International Journal of
Mineralogy, Crystallography, Geochemistry,
Ore Deposits, Petrology, Volcanology
and applied topics on Environment, Archaeometry and Cultural Heritage

Evaluation of the amount of rare earth elements -REE in the Silius fluorite vein system (SE Sardinia, Italy)

Nicola Mondillo [a,*], Giuseppina Balassone [a], Maria Boni [a], Antonio Marino [b], Giuseppe Arfè [a]

[a] Dipartimento di Scienze della Terra, dell'Ambiente e delle Risorse, Università degli Studi di Napoli "Federico II", Complesso Universitario di Monte S. Angelo, Via Cintia 26, 80126, Napoli, Italy
[b] Fluorite di Silius S.p.A. Viale Merello 14, 09023 Cagliari, Italy

ARTICLE INFO

Submitted: January 2017
Accepted: March 2017
Available on line: April 2017

* Corresponding author:
nicola.mondillo@unina.it

DOI: 10.2451/2017PM698

How to cite this article:
Mondillo N. et al. (2017)
Period. Mineral. 86, 121-132

ABSTRACT

The post-Variscan hydrothermal vein system at Silius (Southeastern Sardinia, Italy) is known mostly for its fluorite-barite-galena mineralization, which has been exploited until early 2006 and is now in maintenance. Distinct fluorspar amounts still exist in the mine, and are evaluated at 2 million tonnes of measured resource at 34.5% CaF_2 (727,495 tonnes fluorspar) and 3.2% Pb (67,724 Pb tonnes in galena). Gangue carbonates of the veins, which consist of calcite and ferroan dolomite, contain the REE-minerals synchysite-(Ce) and xenotime. To check the effective amounts of REE in the Silius orebody, representative samples of the carbonate gangue have been collected from several locations in the mine. ICP-MS analyses have been carried out in the samples with the aim to obtain the bulk chemical composition of the carbonates. The concentrations throughout the mine range between 462 and 2,071 ppm (951 ppm on average), mainly consisting of LREE. The average volume of the carbonate gangue still in place, which would be extracted together with fluorite and galena, is currently considered to be around 532,000 tonnes, to which more 750,000 tonnes of carbonates discarded in the old waste dumps may be added. The corresponding total REE amounts currently occurring in the Silius gangue may sum up to 1,220 tonnes pure REE. The discovery of these amounts of REE in the Silius fluorspar mine may open interesting perspectives for the exploration of subeconomic REE concentrations in this type of deposits, where REE could be recovered as by-product of the fluorite exploitation.

Keywords: Critical metals; Critical materials; Fluorite; Rare earth elements; Hydrothermal veins; Sardinia.

INTRODUCTION

A greater variety of metals and minerals have an increasing importance for human development. In addition to the most common metallic elements, like iron and steel alloying elements (e.g. Cr, Ni, W, Mn), base metals (Cu, Zn, Pb), light metals (Al), and precious metals, modern technology relies on virtually all the stable elements of the periodic table, as well as on several "critical" minerals (Graedel et al., 2015). Consequently, there is a growing global concern over the long-term availability of secure and adequate supplies of all these substances needed by contemporary society. Critical metals and minerals (CM), which are those of increasing economic importance that might be susceptible to future scarcity, are a particular worry being vulnerable to politically or economically driven fluctuations in supply (Gunn, 2014). These metals and compounds are essential for high-technology applications. For many of them we have limited

knowledge on how and where they are concentrated in the Earth's crust, how to extract them from their ores, and how to use and dispose of them effectively and safely. At present, the designation of CM applies particularly to the rare-earth elements (REE, from La to Lu, plus geochemically similar Y and Sc), tantalum (Ta), niobium (Nb), lithium (Li), molybdenum (Mo) and indium (In). In what the other critical materials are concerned, which were defined by an expert group chaired by the European Commission of the European Union (EU), the mineral fluorite (fluorspar being its commercial name) was included in the list of 14 raw materials, all labeled as "critical". World resources of fluorspar are approximately 500 million tonnes with proven reserves of 250,000 tonnes (USGS, 2016). Multiple fluorite enterprises in the world are strengthening their integration of upstream and downstream industry chain of fluorite resources for achieving higher added value of products and avoiding unfavorable price influence on fluorite market. However, while current recovery in demand still remains distant in the short term, any upward push for fluorite prices has remained unsuccessful (Salwan, 2016).

The role of REEs, particularly heavy REEs (HREEs), the Tb-Lu portion of the lanthanide series plus Y, in high-tech industries has triggered a worldwide scramble to discover new sources. At present, most REEs are produced from carbonatites and related alkaline rocks, but other sources must also be considered. Simandl (2014) has presented an overview of the geology and market dependency of REE resources. His analysis indicates that changes in Chinese policy have a major impact on the supply and price of REEs. Moreover, the production of these elements is highly dependent upon metallurgical characteristics and the ratio of heavy to light REEs in the ores.

A comprehensive study of REE deposits and occurrences in Europe, based on the results of the EURARE and ASTER projects, has been recently published by Goodenough et al. (2016). Italy does not own economic REE deposits so far, even though several small concentrations have been reported from different host rock types (Boni et al., 2013; Goodenough et al., 2016; Stoppa et al., 2016). Mondillo et al. (2016) reported an interesting occurrence of REE (also including Y) from the Silius hydrothermal vein system in SE Sardinia (Italy), which has been exploited until 2006 for its CaF_2 and Pb resource, and is still significant for the remaining fluorite and galena tonnage. The mine is currently in maintenance and the remaining measured resource is evaluated at 2 million tonnes, at 34.5% CaF_2 (727,495 tonnes of fluorite) and 3.2% Pb (67,724 tonnes Pb in galena) (Fluorite di Silius S.p.A, unpublished report). In this deposit, variable concentrations of mostly REE-bearing fluorocarbonates (synchysite $CaREE(CO_3)_2F$) and subordinate phosphates (YPO_4), have been detected mainly in the carbonate gangue. Considering the "criticality" of both fluorite and REE, the Silius vein system has a double economic significance: 1) for its fluorite resource, and 2) for the contained REEs.

To evaluate the REE average content in the Silius veins, we have conducted a geochemical study on a number of samples representative of the carbonate gangue associated with the remaining fluorite reserves of the mine, which should be treated in any future extraction process aimed to fluorite concentration. In the light of the aforementioned importance of critical metals and minerals, it could be of considerable importance to attempt a recovery of the REEs as byproduct of fluorite extraction.

GEOLOGICAL SETTING OF LATE- TO POST-VARISCAN VEIN DEPOSITS IN SOUTHERN SARDINIA

Regional geological setting

The late- to post-Variscan geological evolution of Europe, as well as part of northern Africa, is characterized by numerous magmatic and hydrothermal mineralizing events, ranging in age from the end of the orogenic compression (Carboniferous) to the onset of Tethys spreading (Triassic-Jurassic). The timing of their emplacement and their characteristics are different from one area to another, but some general features appear to be common (Boni et al., 2002; Muchez et al., 2005; Cheilletz et al., 2010). The Variscan basement of Southern Sardinia is characterized by prevailingly metasedimentary rocks from early Cambrian to early Carboniferous involved in a continental collision and deformed under "very-low" to "low-grade" metamorphic conditions. During the collisional phases, subhorizontal N-S and E-W shortening occurred, and several tectonic units were thrust and imbricated (Conti et al., 2001). Within the Paleozoic successions of Southwestern Sardinia (Figure 1), two tectonostratigraphic units were recognized: 1) an "autochthonous" unit, mainly dominated by sedimentary lithotypes including carbonate sequences; 2) an "allochthonous" unit, consisting of mainly clastic sedimentary rocks, with intercalations of coeval magmatites (Arburese unit, Carmignani et al., 1994). The "allochthonous" successions (also called "External Nappe Zone") are dominant in southeastern Sardinia (Sarrabus-Gerrei), where they have a higher metamorphic grade than the southwestern successions. These mainly siliciclastic sedimentary rocks, are unconformably capped by metarhyolites (the so called "Porfiroidi"), and have been grouped in the San Vito and Solanas formations (Sarrabus) and in the Gerrei unit, respectively (Upper Cambrian-Ordovician; Carmignani et al., 1994). In southeastern Sardinia the emplacement of several granitoid plutons (310-280 Ma, Di Vincenzo et al., 1994 and references therein) followed the Variscan collisional events.

The majority of the late- to post-Variscan mineralized

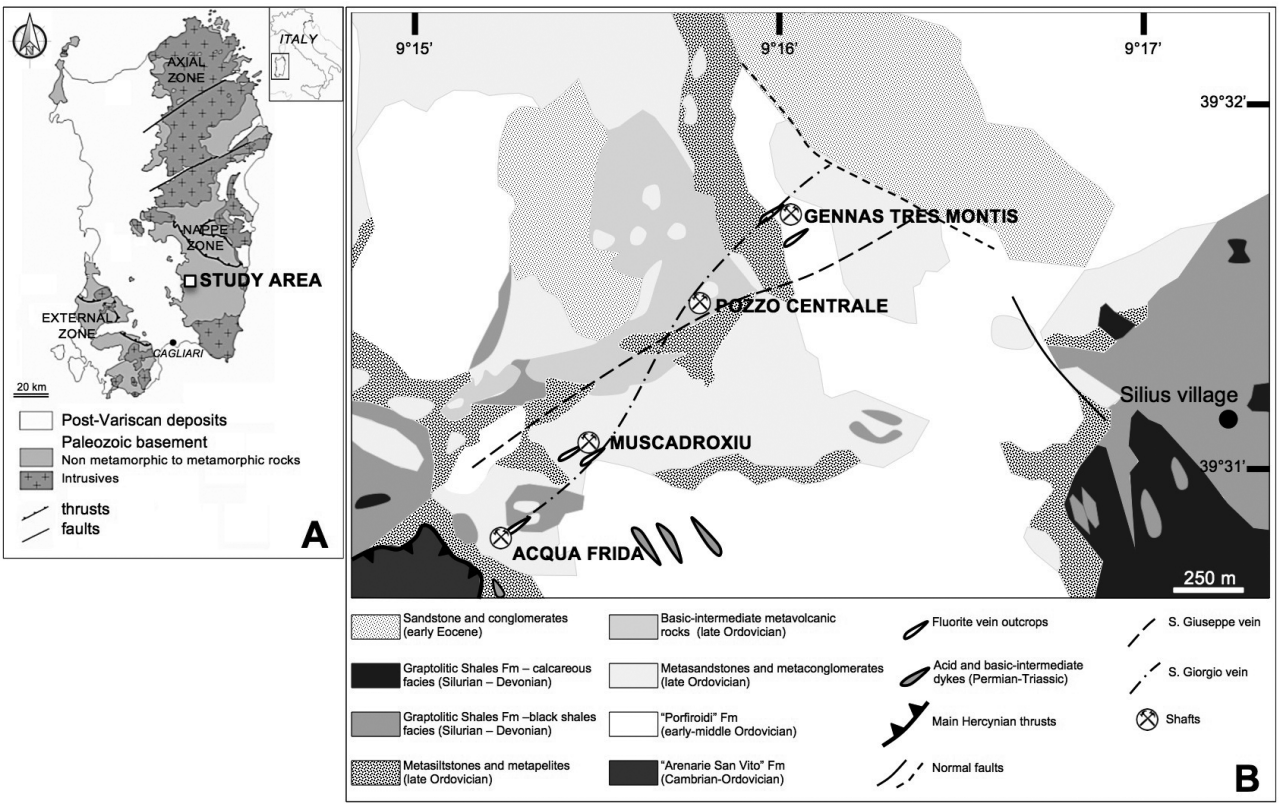

Figure 1. A) Geological sketch map of Southern Sardinia with the location of the Southeastern mining district (Carmignani et al., 1994, modified). B) Simplified geological map of the Silius area (Fluorite di Silius S.p.A., modified).

deposits in southwestern Sardinia (sphalerite, Ag-galena, fluorite and barite) can be attributed to vein- and palaeokarst-types (Boni et al., 2009). For what concerns the southeastern part of the island, hydrothermal mineralizations like the "Filone argentifero" (=Silver Vein) of the Sarrabus district (Valera, 1974; Belkin et al., 1984), and other Paleozoic-hosted ores (Castorina et al., 2008), are mostly within shear zones (Carmignani et al., 1978; Funedda et al., 2011). The Silius vein system (Natale, 1969; Boni et al., 2009), where the exploited minerals consisted of an association of fluorite (prevailing), galena and barite (currently exhausted), is one of the most significant mineralizations in the Gerrei mining region (Figure 1).

The Silius hydrothermal vein system

The Silius vein system crops out discontinuously for 2-3 km along a NE-SW strike, between the Acqua Frida area (39°30'46''N-9°15'05''E), the Muscadroxiu shaft (39°31'00''N-9°15'18''E) and the Genna Tres Montis shaft (39°31'3''N-9°16'00''E), at an elevation ranging between 600 and 700 m a.s.l. (Figure 2). At the 400 m level, the veins reach a maximum length of 4 km. The Silius veins have been mined from the surface (around 600 m a.s.l.) down to 200 m a.s.l., and explored to 100 m a.s.l. The system consists of two main veins, called "San Giorgio" and "San Giuseppe", which have an almost vertical dip (about 75°), and a strike of N-045-E along the main sector Acqua Frida - Genna Tres Montis, and N-065-E northeastward from Genna Tres Montis. These two veins are almost parallel in the topmost levels, with a spacing of 70 m on average, but coalesce at a depth of 350 m a.s.l. in the NE sector, and at a depth of 450 m a.s.l. in the SW sector of the mineralized area. The San Giorgio vein was the first to be formed, and was displaced and brecciated by the San Giuseppe vein. The San Giorgio vein contains bands of chalcedony, pink fluorite, barite and calcite. The San Giuseppe vein is also banded and shows several generations of fluorite, carbonate minerals (mainly sparry calcite), galena and quartz. The width of the veins ranges between 7-8 m in outcrop and 15-20 m in depth, where they are interconnected. The upper part of the vein system contains fluorite, barite and galena with grades of 35%, 10% and 3%, respectively, whereas in the lower zones the amount of barite decreases dramatically and the fluorite and galena grades can reach 50% and 6%, respectively (Natale, 1969; Mondillo et al., 2016). The currently calculated measured resource of fluorite is just

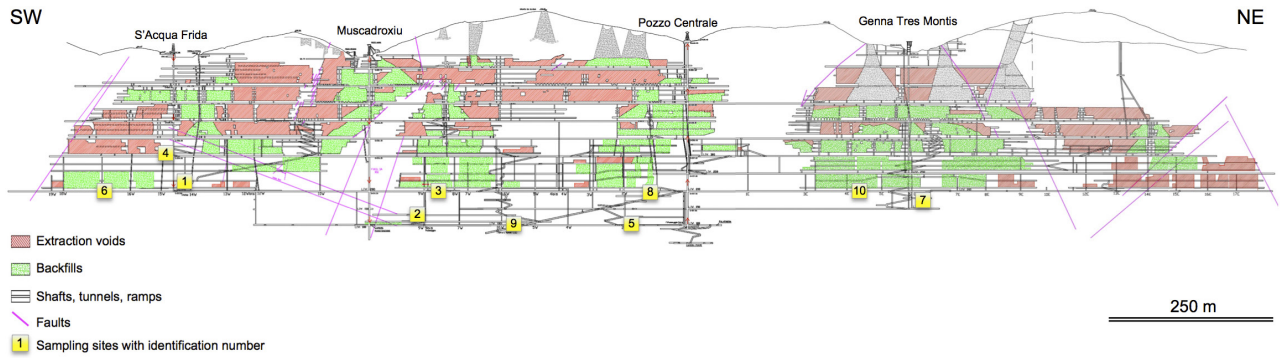

Figure 2. Section along the vein system, showing the sampling points within the Silius mine, with the related sample numbers (Fluorite di Silius S.p.A., modified).

above 2 million tonnes (ore grade averaging 34.5% CaF_2 with 3.2% Pb). The amount and location of the reserves ready to be exploited are presented in Table 1.

The mineralized veins are mainly hosted by the "Porfiroidi" Formation and sporadically by Upper Ordovician sedimentary rocks of the Graptolitic Shales Formation. The fluorite-barite mineralized veins cut locally the late- to post-Variscan (Permian to Triassic felsic and mafic-intermediate) magmatic dykes: this relationship defines a relative minimum age for the mineralization process (Castorina et al., 2008). Microthermometric measurements carried out on fluid inclusions in fluorite and calcite from the San Giorgio and San Giovanni veins (Boni et al., 2009) led to conclude that at least two fluids circulated during the mineralizing event(s) at Silius. The first one was a NaCl±$CaCl_2$ fluid, trapped in primary fluid inclusions from both veins, which precipitated mainly fluorite in the 120-150 °C temperatures range. The second fluid circulated after the main fluorite deposition, and precipitated mainly calcite at temperatures in the 130-180 °C range. The salinity of this fluid can only be estimated (0-18 wt% NaCl equiv.), due to the undiscernible overlap of

Table 1. Amount of fluorspar, lead and carbonates in the measured resources of the Silius mine (Fluorite di Silius S.p.A.).

	Commodity (%)		Carbonate Gangue (%)	Measured Resources
Site	CaF_2	Pb		Tons
above +200 m level				
Acqua Frida shaft west	30.5	7.0	36.0	104,819
Acqua Frida shaft east	38.0	3.0	30.0	45,012
Muscadroxiu shaft west	35.0	3.5	22.0	8,184
Muscadroxiu shaft east	38.6	1.0	15.0	24,576
Centrale shaft west	35.7	1.6	12.0	17,958
below +200 m level				
Acqua Frida shaft west	34.7	4.8	28.5	357,504
Muscadroxiu shaft east	36.8	3.2	19.3	306,956
Centrale shaft west	35.0	1.3	10.0	109,973
Genna Tres Montis west	30.0	2.0	35.0	134,044
Genna Tres Montis east/1	30.0	3.0	32.8	105,400
Genna Tres Montis east/2	36.9	3.0	26.9	503,828
Muscadroxiu shaft east	33.3	2.7	15.0	261,618
Centrale shaft west	30.9	1.3	24.8	127,199
Total	34.5	3.2	25.3	2,107,069

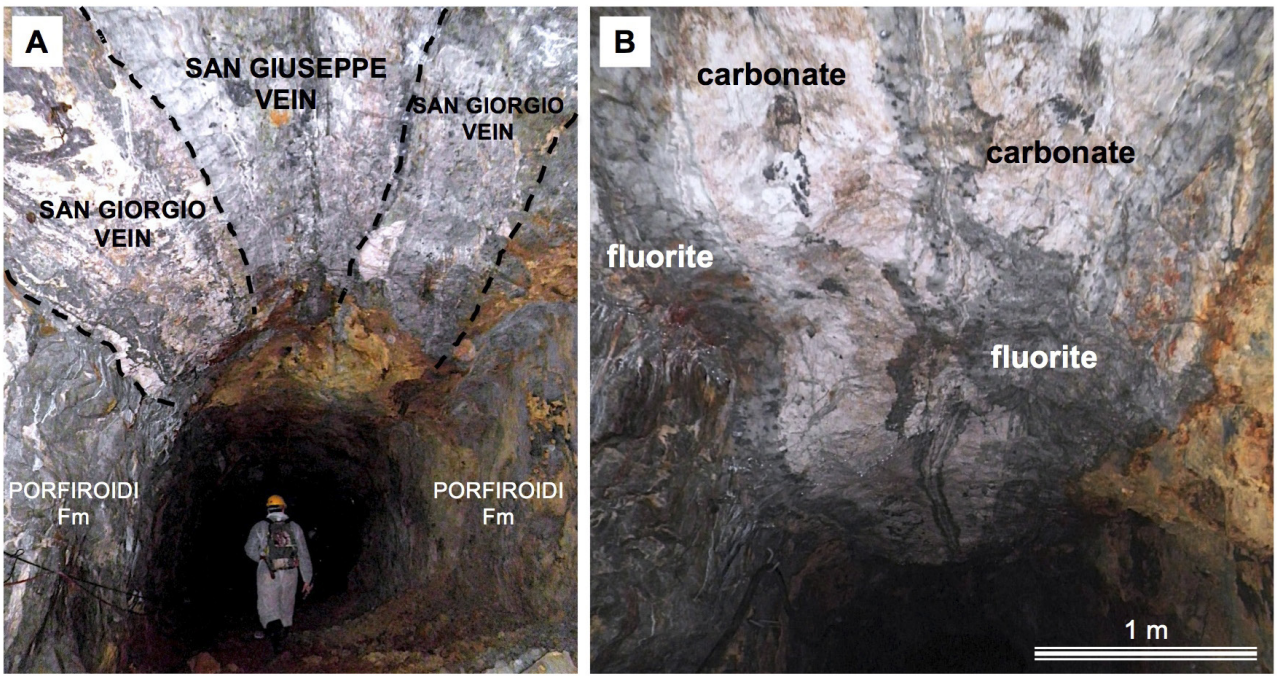

Figure 3. A) The San Giorgio and San Giuseppe mineralized veins cutting the Porfiroidi Fm host rocks; B) Fluorite and carbonate gangue in the San Giuseppe vein.

several generations of fluid inclusions (Boni et al., 2009).

Gangue carbonates containing REE-bearing minerals from both mineralized veins (Figure 3) are composed of a mixture of calcite (prevailing) and dolomite/ferroan dolomite. Under SEM-BSE observation the dolomite, which consists of several ferroan varieties locally approaching ankerite composition, replaces calcite in patches (Figure 4a) (Mondillo et al., 2016). As already demonstrated by Mondillo et al. (2016), Silius carbonates are generally far more enriched in REE than fluorites, with the exception of the last (and least volumetric relevant) fluorite generation, which shows a moderate REE concentration. The most common REE mineral is the fluorocarbonate synchysite-(Ce), with an average formula corresponding to: $Ca_{1.07}(La_{0.19},Ce_{0.36},Pr_{0.04},Nd_{0.15},Sm_{0.03},Gd_{0.03},Y_{0.13})(CO_3)_2F$ (Mondillo et al., 2016). This REE fluorocarbonate mainly fills the intergranular porosity in the carbonate matrix (Figure 4 b,c,d,e), and forms aggregates with tabular habit and euhedral laths. The dimension of synchysite aggregates generally varies between ca. 30 and 100 mm. The REE concentrations in synchysite vary to a large extent, i.e. La ranges between 6.58 and 13.03 wt% La_2O_3, Ce occurs in an interval between 15.90 and 21.10 wt% Ce_2O_3, and Y between 2.58 and 8.45 wt% Y_2O_3 (Mondillo et al., 2016). Xenotime-(Y), with minor contents of Dy and Yb (~3 wt%; Mondillo et al., 2016), has been detected only sporadically at Silius, also as void lining among carbonate crystals (Figure 4f).

SAMPLING AND ANALYTICAL METHODS

The materials analyzed in this research were represented by 10 bulk samples of carbonates, collected from both the San Giuseppe and San Giorgio veins, along the two vertical sections of the Muscadroxiu and the Central shafts of the mine (the latter is located between the Muscadroxiu and the Genna Tres Montis shafts), from 100 m a.s.l. up to 290 m a.s.l. (Table 2, Figure 3). Fluorite samples have not been collected for this study, because the REE content in all fluorite generations is fairly low (Mondillo et al., 2016).

From the initial 10 kg of the weighted samples, ca. 1 kg was allocated for mineralogical and geochemical analyses. The samples were first comminuted at a size less than 15 mm, mixed and quartered for successive analytical procedures. Fractions of 100 g for each sample were previously washed with deionized water and then characterized by X-ray diffraction analysis (XRD). The used instrument was a Seifert-GE ID3003 diffractometer (Dipartimento di Scienze della Terra, dell'Ambiente e delle Risorse-DiSTAR, Università degli Studi di Napoli Federico II, Italy) with CuKα radiation, Ni-filtered at 40 kV and 30 mA, 3-80 °2 range, step scan 0.02°, time 10 s/step, and the RayfleX (GE) software package; a silicon wafer was used to check the instrumental setting. The sample holder was a zero-background plate of quartz crystal cut and polished 6° of the c-axis. Twenty grams were pulverized at 200 mesh for whole rock analyses, i.e. major, minor and trace (REE) elements, carried

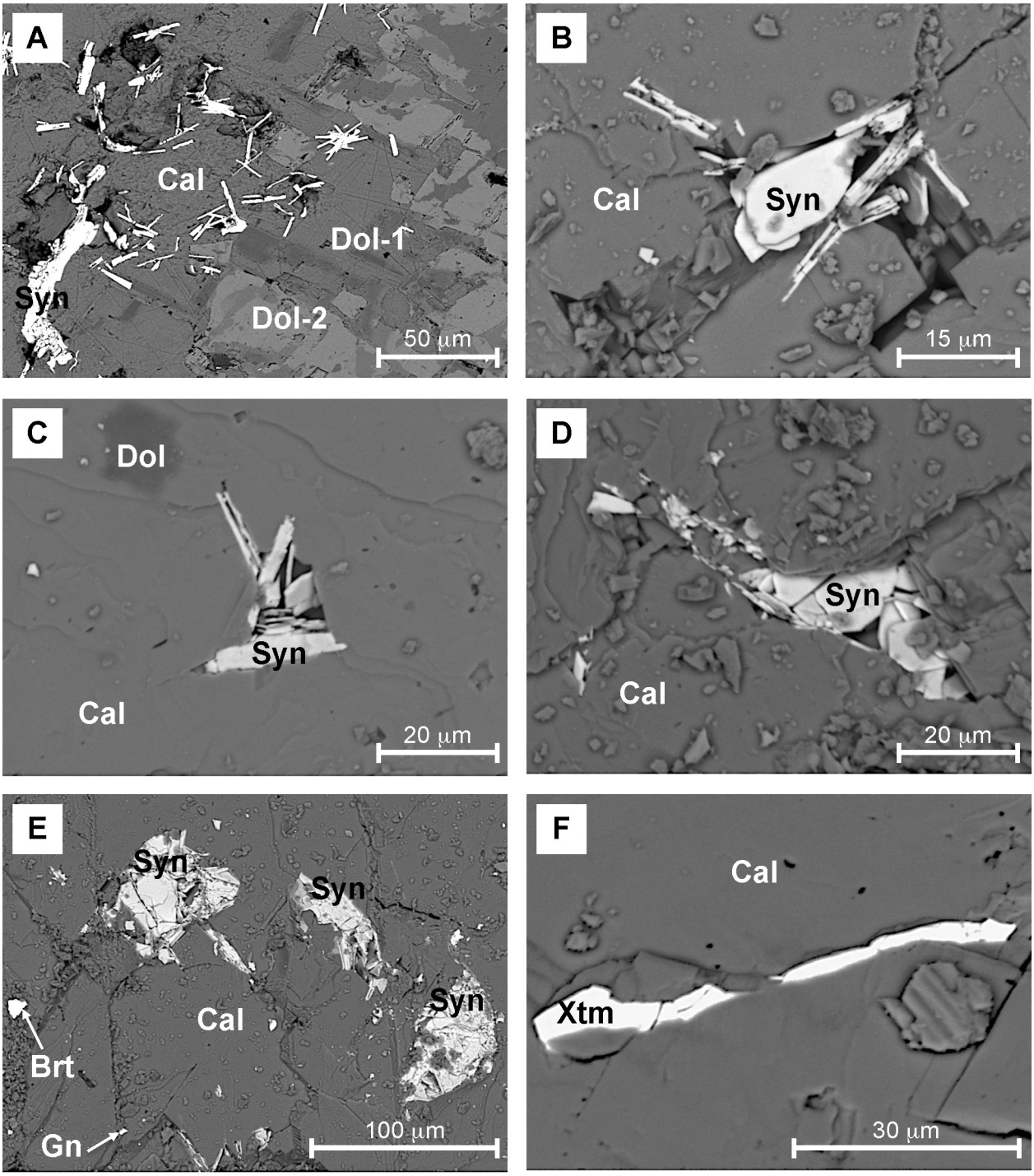

Figure 4. (A) Polished section observed in BSE mode of carbonate gangue (calcite and dolomite) hosting acicular synchysite crystals; SEM micrographs of (B) synchysite euhedral crystals and (C) aggregates occurring as cavity filling in calcite, and (D) subhedral crystal of xenotime cutting across calcite. Brt=barite; Cal=calcite; Dol=dolomite; Gn=galena; Syn=synchysite; Xtm=xenotime.

out at the Bureau Veritas Commodities Canada Ltd. Laboratories (Vancouver, Canada). The protocol LF200 was adopted: major oxides and several minor elements were analyzed by ICP-OES following a $LiBO_2/Li_2B_4O_7$ fusion and dilute nitric digestion. Loss on ignition (LOI) was calculated by weight difference after ignition at 1000 °C. Rare earth and refractory elements were determined by ICP-MS following a $LiBO_2/Li_2B_4O_7$ fusion and nitric

Table 2. Labels and sampling sites of the carbonates from the Silius Mine.

Sample ID	Ore vein	Sampling site
1	S. Giuseppe	2° sublevel 200 Acqua Frida – c/o vertical drift 14 west
2	S. Giuseppe	1° sublevel 100 Muscadroxiu – c/o vertical drift 9 west
3	S. Giorgio	Lev. 200 Muscadroxiu Est, doubled – c/o vertical drift 8-9 west
4	S. Giuseppe	1° sublevel 290 Acqua Frida ovest – c/o S'Acqua Frida shaft
5	S. Giorgio	Lev. 100 Centrale shaft west, doubled – c/o vertical drift 2 west
6	S. Giuseppe	Lev. 200 Acqua Frida west - c/o vertical drift 17 west
7	S. Giuseppe	4° sublevel 100 G.M.T. east - c/o vertical drift 7 east
8	S. Giuseppe	Lev. 200 Centrale shaft west - c/o vertical drift 1west
9	S. Giuseppe	Lev. 100 Centrale shaft Muscadroxiu east - c/o vertical drift 6 west
10	S. Giuseppe	Lev. 200 Centrale shaft east - c/o vertical drift 4-5 east

acid digestion. In addition, a separate volume split was digested in Aqua Regia and analyzed by ICP-MS to detect the precious and base metals.

Selected fragments were then separated from the abovementioned fractions for secondary electron imagining by scanning electron microscopy (SEM) and energy dispersion spectrometry (EDS) investigations. Chips of carbonates, impregnated with Araldite D and Raku Hardener were prepared for polished thin sections EH 2950 (OMT Laboratory, Aosta, Italy). SEM analyses were carried out with a Jeol JSM 5310, equipped with the INCA X-stream pulse processor and the 4.08 version Inca software (Oxford Instruments detector) (DiSTAR, Università di Napoli, Italy), operating at 15 kV primary beam voltage, 50-100 mA filament current, variable spot size and 50 sec net acquisition time. Reference standards were: albite (Si, Al, Na), orthoclase (K), wollastonite (Ca), diopside (Mg), almandine (Fe), rutile (Ti), barite (Ba), strontianite (Sr), eskolaite (Cr), rhodonite (Mn), pyrite (S), sphalerite (Zn), galena (Pb), fluorite (F), apatite (P), sylvite (Cl), smithsonian phosphates (La, Ce, Nd, Sm, Y), pure vanadium (V) and Cornig glass (Th, U). Analytical errors are 1% rel. for major elements and 3% rel. for minor elements.

RESULTS

SEM observations of several carbonate chips from the sampling sites have confirmed that synchysite and less xenotime are widespread in all samples.

Chemical analyses carried out on the bulk carbonate samples are reported in Table 3. Most of the samples show CaO amounts in the range between 51.02 and 54.78 wt%, whereas three samples (no. 6, 8 and 10) have lower CaO contents (33.37-48.36 wt%), compensated by higher amounts of MgO and Fe_2O_3, and, only in sample 8, of SiO_2 likely attributable to quartz and the (variably ferroan) dolomite. Fluorine content up to 2.60 wt% can be ascribed to trace fluorite intergrown with carbonates. Among minor elements, remarkable concentrations of Zn (max 3,553 ppm), Pb (max 3,091 ppm) and Ba (max 3,795 ppm) are due to small intergrowths of sphalerite, galena and barite, typical of the Silius ore. Considering the $(La/Yb)_n$ ratio (Table 3), this is >1 for samples no. 1, 2, 3, 4, 6, 7 and 8; samples 5 and 10 have a $(La/Yb)_n$ ratio slightly above or close to 1, whereas samples 3 and 9 are slightly enriched in HREE ($(La/Yb)_n$ ratio <1; Table 3). This geochemical behavior of REE can also be observed in the diagram normalized to PAAS of Figure 5; the observed pattern is very similar to that of Mondillo et al. (2016), with quite comparable LREE/HREE ratios and positive anomalies of Eu and Y in most of the samples. Samples no. 6, 7 and 8 show the highest amounts of REE (Table 3). In particular, sample no. 7 is the richest one in LREE+Y, with Ce attaining 687 ppm, La 321 ppm, Nd 319 ppm and Y 313 ppm. The total concentrations in REE can be observed in the histograms of Figure 6. The values are in the range of 462-2,071 ppm (951 ppm on average). Samples 6, 7 and 8 reach a total REE amount of 1,369, 2,071 and 1,032 ppm respectively. This means that the REE amounts in the Silius carbonate gangue can locally rise from trace to minor constituents (according to the analytical geochemistry, minor elements concentrations are between 0.1 and 1.0%, and trace elements are less than 0.1%; see for instance Gill, 2014). This confirms the results of Mondillo et al. (2016), who found in the carbonates a slightly lower total REE+Y concentration range of 218-1,846 ppm, with an average value of 944 ppm (Figure 6). The different REE amounts could not be assigned to distinct parts of the mine (above or below the -200 level, north or south), though higher values preferentially occur in the San Giuseppe vein. For sake of comparison, Figure 6 shows also the total REE contents detected in fluorite by Mondillo et al. (2016), this

Table 3. Whole rock analyses of the investigated carbonate samples (see Figure 2 for sample location).

Sample ID	1	2	3	4	5	6	7	8	9	10
CaO (wt. %)	54.21	51.02	53.77	51.37	54.78	48.36	52.46	33.73	52.08	42.10
SiO_2	1.69	4.09	2.79	5.96	3.52	1.91	1.05	13.15	4.58	1.57
$A_{l2}O_3$	0.10	0.03	0.03	0.12	0.05	0.02	0.01	0.12	0.26	0.09
Fe_2O_{3t}	0.45	0.68	0.67	0.40	0.42	2.55	2.27	3.52	0.65	4.18
MnO	0.86	0.79	0.74	0.75	0.49	0.92	0.87	0.97	0.58	1.12
MgO	0.12	1.28	0.19	0.08	0.08	3.72	2.06	9.57	0.23	7.62
Na_2O	0.02	0.01	–	0.01	–	0.02	0.01	0.03	0.02	0.02
K_2O	0.04	–	–	0.04	0.01	–	–	0.04	0.04	0.02
LOI	42.4	41.9	41.5	41.1	40.2	41.5	40.8	37.9	41.3	42.9
Sum	99.89	99.80	99.69	99.83	99.55	99.00	99.53	99.03	99.74	99.62
F	0.16	0.31	0.49	0.48	2.48	1.45	2.60	1.22	0.32	0.95
Be (ppm)	–	–	–	–	–	–	–	2	–	–
Sc	–	2	2	–	11	–	2	4	14	4
V	–	–	–	–	–	–	–	–	10	–
Co	0.4	0.2	0.7	0.3	0.5	0.5	0.7	0.8	0.9	0.9
Ni	–	1.0	0.6	0.9	0.9	0.5	0.7	3.6	1.9	1.4
Cu	9.9	3.9	2.4	3.2	20.1	4.8	20.8	8.8	26.4	14.9
Zn	85	89	124	257	60	615	409	3553	213	1103
Ga	0.9	0.8	0.7	0.9	–	0.7	0.8	1.5	–	1.1
As	1.0	–	13.1	1.0	0.9	–	–	2.6	1.6	1.0
Se	–	–	–	–	–	–	0.9	–	–	0.5
Rb	1.5	0.4	0.3	1.7	0.5	0.3	0.1	1.4	1.7	0.5
Sr	86.4	46.9	141.8	66.4	36.0	77.4	80.2	59.3	50.6	38.4
Zr	1.2	1.0	0.6	1.3	0.4	0.9	0.4	1.8	1.1	1.7
Nb	0.3	0.2	–	–	–	–	–	–	–	–
Mo	0.1	–	0.2	–	0.1	–	–	0.3	–	0.1
Ag	–	–	–	–	0.4	0.6	0.3	–	–	0.4
Cd	0.6	0.2	0.8	2.8	0.4	5.8	3.4	13.8	2.2	5.6
Sn	2	–	4	4	–	–	1	–	1	–
Sb	0.2	0.2	2.2	0.2	0.7	1.3	0.3	0.4	0.3	0.5
Cs	–	–	–	0.1	–	–	–	–	–	–
Ba	347	75	1588	193	90	3795	507	1336	522	363
W	–	–	–	–	–	–	6.2	–	–	–
Au§	1.3	–	–	–	–	–	–	0.5	–	–
Hg	0.03	–	0.08	–	–	0.01	0.01	–	–	0.02
Tl	–	0.1	0.6	0.1	–	–	0.3	–	–	–
Pb	136.7	26.6	26.2	45.0	3090.7	2798.1	506.3	141.3	93.5	95.1
Bi	–	–	–	–	–	–	0.6	–	–	–
Th	–	–	0.3	–	0.6	–	–	–	0.7	0.4
U	–	–	0.2	–	0.2	–	0.3	0.4	0.1	0.2
Y	92.1	129.2	136.8	105.9	96.4	206.8	313.0	131.1	139.0	136.1
La	127.6	180.1	57.7	154.3	137.0	269.6	320.7	208.0	141.4	161.1
Ce	200.7	300.6	108.3	249.0	253.4	482.1	686.7	367.6	270.6	298.5
Pr	20.8	32.3	12.8	24.8	27.1	51.8	81.8	39.7	28.6	32.2
Nd	76.8	120.2	49.9	91.9	97.4	191.3	318.8	151.8	103.4	119.8
Sm	14.5	23.6	13.9	16.6	22.3	40.4	93.3	31.6	25.1	26.3
Eu	12.8	15.5	6.1	14.6	6.7	23.4	33.1	17.3	8.0	14.3
Gd	17.6	27.0	17.3	20.4	23.1	48.3	103.9	35.0	28.2	31.9
Tb	2.4	3.7	3.4	2.7	3.7	6.1	14.9	4.5	5.0	4.6
Dy	13.2	19.9	22.5	13.9	19.7	29.1	66.0	23.2	28.9	23.5
Ho	2.3	3.4	4.4	2.3	3.3	4.4	9.2	3.7	5.3	4.0
Er	5.8	8.6	13.0	5.7	9.3	9.8	18.0	9.5	14.7	10.7
Tm	0.7	1.2	1.9	0.6	1.3	1.0	1.8	1.2	2.2	1.5
Yb	3.4	6.6	12.0	2.8	9.4	4.5	9.1	7.1	14.3	9.4
Lu	0.5	0.9	1.7	0.3	1.4	0.6	1.1	1.0	2.0	1.3
Eu/Eu*	3.78	2.90	1.86	3.74	1.38	2.49	1.58	2.44	1.41	2.33
Ce/Ce*	0.87	0.88	0.89	0.90	0.93	0.91	0.95	0.90	0.95	0.93
(La/Yb)n	2.78	2.03	0.36	4.01	1.08	4.43	2.61	2.16	0.73	1.26

Fe_2O_{3t}=Fe as total iron; bdl=below detection limit; §=ppb; Eu/Eu*=[Eun/√(Smn •Gdn)], where the subscript n stands for values PAAS normalized; Ce/Ce*=[Cen/√(Lan •Prn)]; (La/Yb)n=Lan/Ybn.

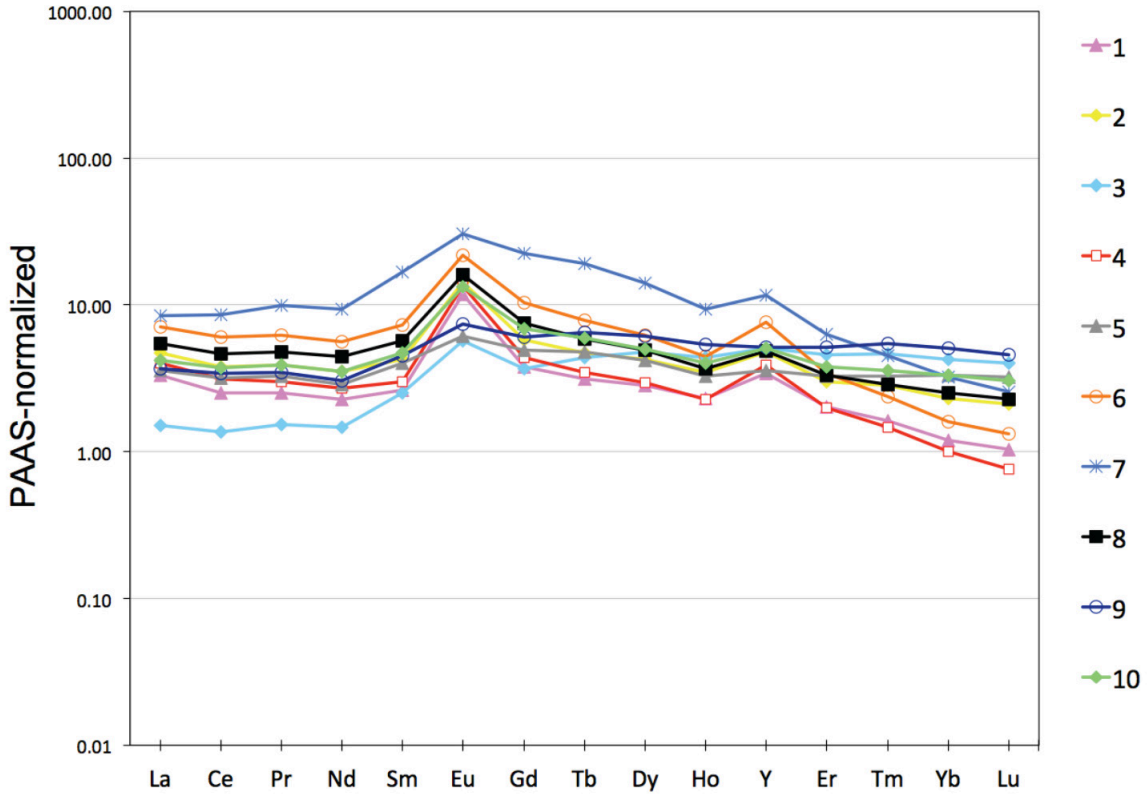

Figure 5. REE concentrations in bulk carbonate samples, normalized to PAAS (post-Archean Australian Shale; Taylor and McLennan, 1985).

demonstrating that the total REE amount always represents only a trace component of the fluorite ore (max 627 ppm, 212 ppm on average).

DISCUSSION AND CONCLUSIONS

The Silius mineralization has always been described as a vein system containing a simple association of fluorite, barite and galena with a gangue consisting of calcite and quartz (Natale, 1969; Castorina et al., 2008; Boni et al., 2009). The presence of synchysite and xenotime reveals that this gangue could be relevant for its REE contents (Mondillo et al., 2016). Synchysite (the main REE-carrier in the Silius fluorite veins) is generally found associated with orthomagmatic-hydrothermal or hydrothermal-metasomatic REE-mineralizations, but it has been also found in Alpine-type veins (Gieré, 1996, and references therein; Williams-Jones et al., 2000; Förster, 2001; Chakhmouradian and Wall, 2012; Augé et al., 2014). This mineral was detected in post-Variscan hydrothermal veins in Germany (e.g. Harz Mountains and Schwarzwald), where it is associated with bastnäsite (Gieré, 1996, and references therein; Haack et al., 1987; von Gehlen et al., 1986). According to Augè et al. (2014), most synchysites described in the literature are considered to be late- to post-magmatic, and are developed at the expense of pre-existing REE minerals: synchysite is seldom the only REE mineral present in these deposits and mainly forms complex associations with bastnäsite, parisite, rhabdophane and cerianite. In the Tundulu carbonatite complex in Malawi synchysite is the only REE fluorocarbonate in the calcite of the carbonatite, whereas synchysite is coexisting with parisite in the ankerite part of the complex (Ngwenya, 1994). The Tundulu veins consist of up to 98% calcite crystals with accessory synchysite that may be interstitial to calcite. The Malawi occurrence presents strong similarities to the synchysites detected in the amygdules from the Reyran basalts (Esterel, France), reported by Augè et al. (2014), where synchysite is the only REE mineral identified. In the Reyran amygdules there is no evidence of crystallization of this fluorocarbonate at the expense of pre-existing REE minerals, this suggesting a direct crystallization from a fluid in open voids. This texture is very similar to that observed at Silius, where synchysite forms euhedral crystals in cavities, cemented by late fluorite phases (Mondillo et al., 2016). Xenotime is a common accessory phase in granites and pegmatites and is a common detrital mineral in siliciclastic sedimentary rocks; however, it may also form during hydrothermal

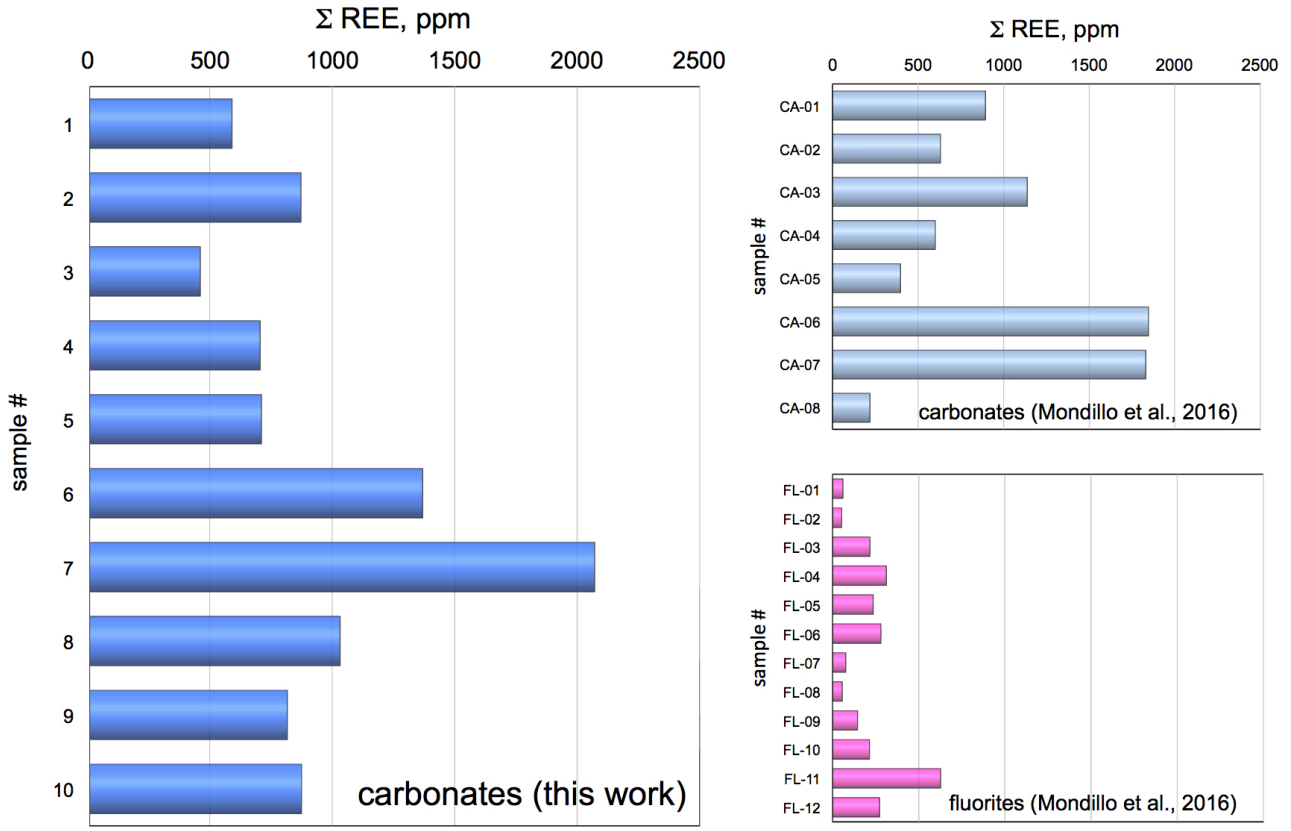

Figure 6. Histograms reporting the total REE (plus Y) contents in the investigated samples.

processes (Brown et al., 2002; Kositcin et al., 2003; Schaltegger et al., 2005; Cook et al., 2013). In the Silius paragenesis, xenotime has been detected in association with synchysite (Mondillo et al., 2016).

REE geochemistry of carbonates in Variscan fluorite veins has been widely investigated, not only in the deposits of the Harz mountains in Germany (Möller et al., 1984; Bau and Möller, 1992), but also in the occurrences of the Valle de Tena in Spain (Subías and Fernández-Nieto, 1995), and in the El Hammam orebodies in Morocco (Cheilletz et al., 2010; Zemri et al., 2015). At the moment none of the above deposits has been considered economic for REEs extraction.

As reported before, Silius measured resources are currently evaluated at 2 million tonnes at 34.5% CaF_2 and 3.2% Pb (as assessed by Fluorite di Silius S.p.A). The veins also contain 532,000 tonnes of carbonates (25.3% of the bulk extractable material) (see Table 1). Considering the average REE concentrations (951 ppm) in the carbonates, we have calculated that in Silius mine a total REE amount of 505 tonnes could be present. So far the carbonates (calcite+ferroan dolomite) together with quartz, have been considered useless gangue that, after the concentration of fluorite and galena by way of flotation, was discarded into barren dumps. In fact, during the 40 years of exploitation of the mine, about 2,700,000 tonnes of sandy material and 2,000,000 tonnes of muds have been accumulated near the Assemini treatment plant (Cagliari). This material consists mainly of a mixed minerals gangue, where the carbonate values range between 15% and 17%.

These amounts sum to about 750,000 tonnes of total carbonates where, considering again the calculated average REE concentration of 951 ppm, a valuable REE amount around 710 tonnes could be present. The corresponding total REE amounts currently related to Silius may sum up to 1,220 tonnes.

In our opinion, the discovery of discrete amounts of REE in the Silius fluorite mine, added to their probable content in the discarded material from the flotation plant may open interesting perspectives for the exploration of subeconomic REE concentrations in this type of post-Variscan hydrothermal deposits, where REE might be eventually recovered as by-product of the fluorite exploitation.

In conclusion, it is possible to attribute to the Silius mineralization a "double critical" significance, based not only on its fluorite content, but also on the possibly recoverable REE amounts contained in the carbonate gangue. A pilot study on the economic processing of the

REE minerals from the Silius Run of The Ore and from the dumps materials would be the next necessary step. From the exploration point of view, further work should consist in an accurate screening of several post-Variscan veins occurring in southeastern Sardinia (e.g. the Filone Argentifero of the Sarrabus district), in order to check the possible content of REE minerals in their carbonate gangue.

ACKNOWLEDGEMENTS

We would like to thank Ing. G. Mura, Director of the Silius mine, for having allowed us to sample in the underground levels and R. de' Gennaro (DiSTAR, Napoli) for the SEM-EDS analyses. We are indebted to two anonymous reviewers, whose comments have highly enhanced the quality of the manuscript.

REFERENCES

Augé T., Bailly L., Wille G., 2014. An unusual occurrence of synchysite-(Ce) in amygdales from the Esterel volcanic rocks, France: implications for rare-earth element mobility. Canadian Mineralogist 52, 837-856.

Bau M. and Möller P., 1992. Rare earth element fractionation in metamorphogenic hydrothermal calcite, magnesite and siderite. Mineralogy and Petrology 45, 231-246.

Belkin H.E., De Vivo B., Valera R., 1984. Fluid inclusion study of some Sarrabus fluorite deposits, Sardinia, Italy. Economic Geology 79, 409-414.

Boni M., Muchez Ph., Schneider J., 2002. Permo-Mesozoic multiple fluid flow and ore deposits in Sardinia: a comparison with Post-Variscan mineralisation of Western Europe. In: The timing and location of major ore deposits in an evolving orogen. (eds.) D. Blundell, F. Neubauer, A. von Quadt, Geological Society, London, Special Publications 206, 199-211.

Boni M., Balassone G., Fedele L., Mondillo N., 2009. Post-Variscan hydrothermal activity and ore deposits in southern Sardinia (Italy): selected examples from Gerrei (Silius vein system) and Iglesiente district. Periodico di Mineralogia 78, 19-35.

Brown S.M., Fletcher I.R., Stein H.J., Snee L.W., Groves D.I., 2002. Geochronological constraints on pre-, syn-, and post-mineralization events at the world-class Cleo gold deposit, Eastern Goldfields province, Western Australia. Economic Geology 97, 541-559.

Carmignani L., Oggiano G., Pertusati P.C., 1994. Geological outlines of the Hercynian basement of Sardinia. In: Petrology, Geology and Ore deposits of the Paleozoic Basement of Sardinia, Guidebook to the B3 field excursion. 16th General Meeting of the International Mineralogical Association, Pisa, pp. 9-20.

Carmignani L., Oggiano G., Barca S., Conti P., Salvadori I., Eltrudis A., Funedda A., Pasci S., 2001. Geologia della Sardegna, Note illustrative della Carta Geologica della Sardegna alla scala 1:200.000. Memorie Descrittive Carta Geologica d'Italia, Servizio Geologico Italiano, 60, Istituto Poligrafico Zecca dello Stato, Roma, pp 283.

Castorina F., Masi U., Padalino G., Palomba M., 2008. Trace-element and Sr-Nd isotopic evidence for the origin of the Sardinian fluorite mineralization (Italy). Applied Geochemistry 23, 2906-2921.

Chakhmouradian A.R. and Wall F., 2012. Rare earth elements: minerals, mines, magnets (and more). Elements 8, 333-342.

Cheilletz A., Gasquet D., Filali F., Archibald D.A., Nespolo M., 2010. A late Triassic $^{40}Ar/^{39}Ar$ age for the El Hammam high-REE fluorite deposit (Morocco): mineralization related to the Central Atlantic magmatic province? Mineralium Deposita 45, 323-329.

Conti P., Carmignani L., Funedda A., 2001. Changing of nappe transport direction during the Variscan collisional evolution of central-southern Sardinia (Italy). Tectonophysics 332, 255-273.

Cook N.J., Ciobanu C.L., O'Rielly D.,Wilson R., Das K., Wade B., 2013. Mineral chemistry of rare earth element (REE) mineralization, Browns Ranges, Western Australia. Lithos 172-173, 192-213.

Di Vincenzo G., Elter F.M., Ghezzo C., Palmeri R., Ricci C.A., 1994. Petrological evolution of the Palaeozoic basement of Sardinia. In: Petrology, Geology and Ore Deposits of the Palaeozoic Basement of Sardinia. (eds.): L. Carmignani, C. Ghezzo, A. Marcello, P.C. Pertusati, S. Pretti, C.A. Ricci, I. Salvadori, Guide Book to the Field Excursion 145, pp. 643-658.

Förster H.J., 2001. Synchysite-(Y) ± synchysite-(Ce) solid solutions from Markersbach, Erzgebirge, Germany: REE and Th mobility during high-T alteration of highly fractionated aluminous A-type granites. Mineralogy and Petrology 72, 259-280.

Funedda A., Naitza S., Conti P., Dini A., Buttau C., Tocco S., Carmignani L., 2011. Structural control of ore deposits: the Baccu Locci shear zone (SE Sardinia). Rendiconti Online Società Geologica Italiana 15, 66-68.

Gieré R., 1996. Formation of rare earth minerals in hydrothermal systems. In: Rare Earth Minerals: Chemistry, Origin and ore Deposits. (eds.): A.P. Jones, F. Wall, C.T. Williams, Mineralogical Society Series 7. Chapman and Hall, London, 105-150.

Gill R., 2014. Modern Analytical Geochemistry: An introduction to quantitative chemical analysis techniques for earth, environmental and materials scientists. Routledge, New York, 342 pp.

Goodenough K.M., Schilling J., Jonsson E., Kalvig P., Charles N., Tuduri J., Deady E.A., Sadeghi M., Schiellerup H., Müller A., Bertrand G., Arvanitidis N., Eliopoulos D.G., Shaw R.A., Thrane K., Keulen N., 2016. Europe's rare earth element resource potential: An overview of REE metallogenetic provinces and their geodynamic setting. Ore Geology Reviews 72, 838-956.

Graedel T.E., Harper E.M., Nassar N.T., Nuss P., Reck B.K., 2015. Criticality of metals and metalloids. PNAS 112-14, 4257-4262.

Gunn G. (Ed.), 2014. Critical Metals Handbook. American Geophysical Union, ISBN 978-0-470-67171-9, 454 p.

Haack U., Schnorrer-Köhler G., Lüders V., 1987. Seltene Erdminerale aus hydrothermalen Gängen des Harzes. Chemie der Erde 47, 41-45.

Kositcin N., Mc Naughton N.J., Griffin B.J., Fletcher I.R., Groves D.I., Rasmussen B., 2003. Textural and geochemical discrimination between xenotime of different origin in the Archaean Witwatersrand Basin, South Africa. Geochimica et Cosmochimica Acta 67, 709-731.

Möller P., Morteani G., Dulski P., 1984. The origin of the calcites from Pb-Zn veins in the Harz mountains, Federal Republic of Germany. Chemical Geology 45, 91-112.

Mondillo N., Boni M., Balassone G., Spoleto S., Stellato F., Marino A., Santoro L., Spratt J., 2016. Rare earth elements (REE)-Minerals in the Silius fluorite vein system (Sardinia, Italy). Ore Geology Reviews, 74, 211-224.

Muchez P., HeijlenW., Banks D., Blundell D., Boni M., Grandia F., 2005. Extensional tectonics and the timing and formation of basin-hosted deposits in Europe. Ore Geology Reviews 27, 241-267.

Natale P., 1969. Il giacimento di Silius nel Gerrei. Bollettino Associazione Mineraria Subalpina 6, 1-35.

Ngwenya B.T., 1994. Hydrothermal rare earth mineralization of the Tundulu Complex, Malawi: processes at the fluid/rock interface. Geochimica et Cosmochimica Acta 58, 2061-2072.

Salwan S., 2016. Competition sees cheaper fluorspar offers. Industrial Minerals, 29 July 2016.

Schaltegger U., Pettke T., Audétat A., Reusser E., Heinrich C.A., 2005. Magmatic-to-hydrothermal crystallization in the W-Sn mineralized mole granite (NSW, Australia) part I: crystallization of zircon and REE-phosphates over three million years - a geochemical and U-Pb geochronological study. Chemical Geology 220, 215-235.

Simandl G., 2014. Geology and market-dependent significance of rare earth element resources. Mineralium Deposita 49, 889-904.

Stoppa F., Pirajno F., Schiazza M., Vladykin NV., 2016. State of the art: Italian carbonatites and their potential for critical-metal deposits. Gondwana Research 37, 152-171.

Subías I. and Fernández-Nieto C., 1995. Hydrothermal events in the Valle de Tena (Spanish Western Pyrenees) as evidenced by fluid inclusions and trace-element distribution from fluorite deposits. Chemical Geology 124, 267-282.

Taylor St.R. and McLennan S.M., 1985. The continental crust: its composition and evolution. Blackwell Scientific Publications Oxford, London, Edinburgh, 312 p.

USGS 2016. Fluorspar. Mineral Commodity Summaries, 62-63.

Valera R., 1974. Appunti Sulla morfologia, termometria e composizione delle inclusion fluide di fluoriti sarde. Rendiconti della Società Italiana di Mineralogia e Petrologia 30, 459-480.

Von Gehlen K., Grauert B., Nielsen H., 1986. REE minerals in southern Schwarzwald veins and isotope studies on gypsum from the central Schwarzwald, F.R. Germany. Neues Jahrbuch für Mineralogie - Monatshefte 9, 393-399.

Williams-Jones A.E., Samson I.M., Olivo G.R., 2000. The genesis of hydrothermal fluorite-REE deposits in the Galllinas Mountains, New Mexico. Economic Geology 95, 327-342.

Zemri O., Bouabdellah M., Jébrak M., Klügel A., Sadequi M., Gaouzi Lou Maacha A., 2015. Geology and REE geochemistry of the El Hammam REE-rich fluorite deposit (Central Meseta, Morocco). Proceedings of the 13th Biennial SGA Meeting on Mineral Resources in a Sustainable World, Nancy, France, 1679-1682.